

## Electronic Supplementary Information (ESI)

### **A Simple Fluorene Core-Based Non-fullerene Acceptor for High Performance Organic Solar Cells**

Suman<sup>a,b</sup>, Anirban Bagui<sup>a</sup>, Ram Dutt,<sup>c</sup> Vinay Gupta<sup>c</sup>, and Surya Prakash Singh<sup>\*a,b</sup>

<sup>a</sup>Inorganic and Physical Chemistry Division, CSIR-Indian Institute of Chemical Technology, Uppal road, Tarnaka, Hyderabad-500007, India

<sup>b</sup>Academy of Scientific and Innovative Research

<sup>c</sup>CSIR-National Physical Laboratory, New Delhi-110012, India

\*Corresponding author: Dr. Surya Prakash Singh

## Contents

General Experimental Details .....	3
S1. Methods and materials .....	3
S2. Synthetic Procedure .....	3
Scheme S1. Synthetic scheme of FRd <sub>2</sub> .....	4
Fig. S1 <sup>1</sup> H NMR of BT-F-Br in CDCl <sub>3</sub> .....	8
Fig. S2 <sup>1</sup> H NMR of F2CHO in CDCl <sub>3</sub> .....	8
Fig. S3 <sup>1</sup> H NMR of FRd <sub>2</sub> in CDCl <sub>3</sub> .....	8
Fig. S4 <sup>13</sup> C NMR of BT-F-CHO in CDCl <sub>3</sub> .....	9
Fig. S5 <sup>13</sup> C NMR of F2CHO in CDCl <sub>3</sub> .....	9
Fig. S6 <sup>13</sup> C NMR of FRd <sub>2</sub> in CDCl <sub>3</sub> .....	10
Fig. S7 MALDI-TOF spectrum of <b>FRd<sub>2</sub></b> .....	10
Fig. S8 FT-IR spectrum of <b>FRd<sub>2</sub></b> .....	11
S3. Optoelectronic properties .....	11
S4. Electrochemical properties .....	12
Fig. S9 (a) Molar extinction coefficient ( $\epsilon$ ), (b) Cyclic Voltammogram of FRd <sub>2</sub> .....	12
Table S1. Optoelectronic properties of <b>FRd<sub>2</sub></b> .....	13
S5. Density Functional Theory calculation .....	13
Table S2. Major allowed transitions for <b>FRd<sub>2</sub></b> in the range of 300-800 nm calculated at B3LYP/6-311g (d,p) level using density functional theory in DCM solvent .....	13
Fig. S10 Distribution of frontier molecular orbitals of <b>FRd<sub>2</sub></b> as estimated by density functional theory calculation at B3LYP level .....	14
S6. Device fabrication .....	14
S7. Charge carrier mobility .....	15
Fig. S11 Mott-Gurney's SCLC fitting to calculate hole and electron mobility of PTB7-Th and SMNFEA in thermally annealed films. ....	15
Table S3. Charge transport parameters of PTB7-Th: <b>FRd<sub>2</sub></b> blend films. ....	15
S8. Photoluminescence Quenching .....	16
Fig. S12 Stern-Volmer plots for PTB7-Th: <b>FRd<sub>2</sub></b> blends obtained from PL quenching experiments. ....	16
S9. GIXRD analysis .....	16
Fig. S13 The GIXRD graphs of thermally annealed and solvent vapor annealed PTB7-Th: <b>FRd<sub>2</sub></b> blend film and pristine PTB7-Th, <b>FRd<sub>2</sub></b> films .....	17
REFERENCES .....	17

## General Experimental Details

### S1. Methods and materials

**S1.1 Materials:** All the starting chemicals and reagents for synthesis were purchase from commercial sources and used without further purification. Fluorene was purchase from Sigma Aldrich and 2,3-diamino benzene was purchase from Alfa Aesar. Solvent were dried and purified by distillation over calcium hydride under nitrogen atmosphere. All solution phase reactions were carried out under nitrogen atmosphere. Column chromatography was carried out on silica gel (60-120 mesh and 100-200 mesh).

**S1.2 General Method:** All intermediates and final molecule were characterized by NMR, MASS and FT-IR spectroscopy.  $^1\text{H}$  NMR and  $^{13}\text{C}$  NMR spectra were recorded in *d*-chloroform on Bruker AV-400 spectrometer and AV-300 NMR spectrometer instrument with tetramethylsilane (TMS) as internal reference at 298 K. Chemical shifts are presented in  $\delta$  (ppm) referenced to solvent residual peak at 7.26 ppm and 77.0 ppm for  $^1\text{H}$  NMR and  $^{13}\text{C}$  NMR, respectively.

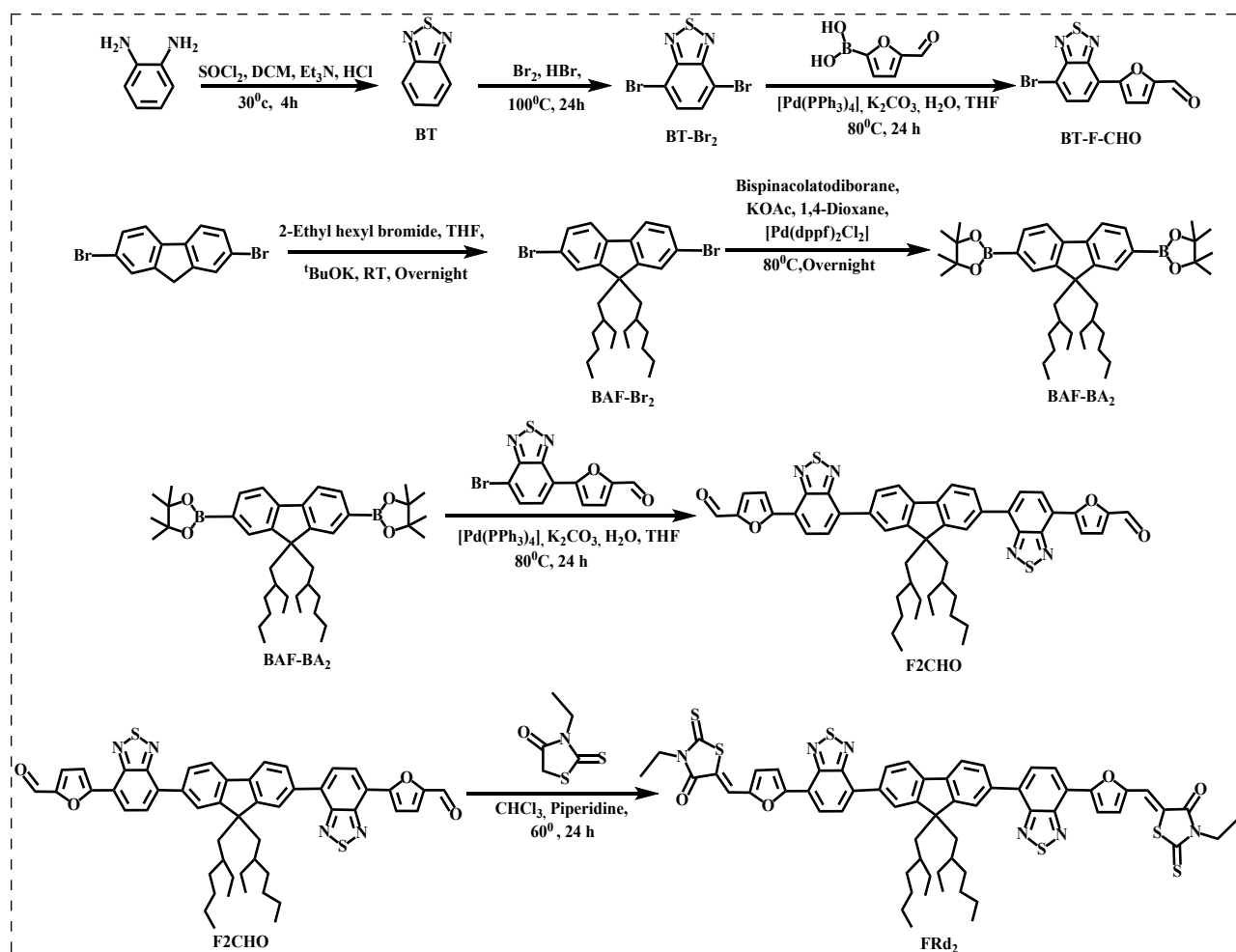
### S2. Synthetic Procedure

The detail synthetic route of **FRd<sub>2</sub>** is described in **Scheme S1**. Intermediate dialdehyde (F<sub>2</sub>CHO) was synthesized by palladium catalyzed Suzuki cross coupling between BAF-BA<sub>2</sub> and BT-F-CHO in 53% yield. The target molecules **FRd<sub>2</sub>** was obtained by Knoevenagel condensation of F<sub>2</sub>CHO intermediate with rhodanine chromophoric. All intermediates and final molecule were fully characterized by  $^1\text{H}$  NMR,  $^{13}\text{C}$  NMR, Fourier transform infrared (FT-IR) spectroscopy and Matrix-assisted LASER desorption/ionization-time-of flight mass spectrometry (MALDI-TOF MS) spectroscopy (**Fig. S1-S8**). New acceptor molecule have good solubility in common organic solvents such as dichloromethane, THF, chloroform and chlorobenzene at room temperature because of presence of branched alkyl chain on fluorene core.

#### **Benzothiadiazole (BT):<sup>1</sup>**

To a 250 mL round bottom flask were added *o*-phenylene diamine (5g, 46.23 mmol), 60 mL of CH<sub>2</sub>Cl<sub>2</sub> and triethylamine (18.72 g, 184.92 mmol). The solution was stirred until total dissolution of the *o*-phenylene diamine. Thionyl chloride (22.2 g, 184.92 mmol) was added drop wise very

slowly and then reaction mixture was refluxed for 4 h. After completion of reaction, reaction mixture was cooled to room temperature. 100 mL of water added was added to the reaction mixture and concentrated HCl was added to a final pH of 2. Organic compound was extracted with DCM and dried over Na<sub>2</sub>SO<sub>4</sub> and filtered. The desired compound was purified by column chromatography with hexane, affording pure compound **BT** in 77% yield (4.8 g, 35.25 mmol). <sup>1</sup>H NMR (400 MHz, CDCl<sub>3</sub>): δ ppm 8.02-7.98 (dd, 2H, J=3.17 Hz.); 7.59-7.56 (dd, 2H, J=3.17 Hz.). <sup>13</sup>C NMR (125.77 MHz, CDCl<sub>3</sub>): δ ppm 154.58; 129.23; 121.66.



**Scheme S1.** Synthetic scheme of FRd<sub>2</sub>.

#### 4,7-Dibromo benzothiadiazole (BTBr<sub>2</sub>): <sup>1</sup>

To a 500 mL two-necked round bottom flask were added benzothiadiazole (4.2 g, 30.84 mmol) and 60 mL of HBr (47%). A solution containing Br<sub>2</sub> (12.32 g, 77.10 mmol) in 20 mL of HBr was added drop wise very slowly. After total addition of the Br<sub>2</sub>, the solution was refluxed for 6 h.

The mixture was allowed to cool to room temperature and sufficient saturated solution of NaHCO<sub>3</sub> added to consume completely any excess Br<sub>2</sub>. The mixture was filtered under vacuum and washed with water. The solid was then washed once with cold Et<sub>2</sub>O and dried under vacuum for 20 h, affording the desired product **BTBr<sub>2</sub>** in 80% yield (7.2 g, 24.49 mmol). <sup>1</sup>H NMR (500 MHz, CDCl<sub>3</sub>): δ ppm 7.73 (s, 2H). <sup>13</sup>C NMR (100.62 MHz, CDCl<sub>3</sub>): δ ppm 152.6; 132.1; 113.6.

#### **5-(7-bromobenzo[c][1,2,5]thiadiazole-4-yl)furan-2-carbadehyde (BT-F-CHO):**

In a 50 ml of two neck round bottom flask a mixture of BT-Br<sub>2</sub> (1 g, 3.40 mmol), 5-formyl furan-2-boronic acid (0.475 g, 3.06 mmol), K<sub>2</sub>CO<sub>3</sub> (2M Solution 5 mL), in THF (30 ml) was degassed for 30 minutes before addition of [Pd (PPh<sub>3</sub>)<sub>4</sub>] (10 mg) and subsequent degassing for 10 min. The reaction mixture was heated under argon at 80 °C for 24 hrs. After cooling to room temperature, the reaction was quenched with water and extracted with CH<sub>2</sub>Cl<sub>2</sub> and dried over Na<sub>2</sub>SO<sub>4</sub> and filtered. The desired compound was purified by column chromatography with hexane, affording pure compound **BT-F-CHO** in 56% yield (0.580 g, 1.876mmol). <sup>1</sup>H NMR (500 MHz, CDCl<sub>3</sub>): δ ppm 9.75-9.74 (s, 1H), 8.16-8.14 (d, J=7.78Hz, 1H), 7.97-7.94 (d, J=7.6Hz, 1H) 7.89-7.87(d, J=3.81Hz, 1H), 7.44-7.42(d, J=3.81Hz, 1H). <sup>13</sup>C NMR (100 MHz, CDCl<sub>3</sub>): δ ppm 177.45, 154.13, 152.05, 132.2, 129.42, 126.23, 125.92, 123.65, 122.37, 115.39, 114.61.

#### **BAF-Br<sub>2</sub>:<sup>2</sup>**

In a 100 ml of two neck round bottom flask a stirred solution of dibromofluorene(2 g, 6.172 mmol) in 30 mL THF under nitrogen was added t-BuOK (2.077 g, 18.51 mmol) in 20 ml THF slowly at 0 °C. After 1 h, 2-ethylhexyl bromide (3.57 g, 18.51 mmol) was added to the reaction mixture and stirred at room temperature for 8 hours. The reaction mixture was filtered and the solvent was removed under reduced pressure. The organic compound was extracted with CH<sub>2</sub>Cl<sub>2</sub> and dried over Na<sub>2</sub>SO<sub>4</sub>. The desired compound was purified by column chromatography with hexane, affording oily product **BAF-Br<sub>2</sub>** in 71% yield (2.4 g, 4.376 mmol). <sup>1</sup>H NMR (400 MHz, CDCl<sub>3</sub>):δ ppm d 7.52–7.50 (d, J=7.83Hz, 2H), 7.45–7.44 (d, J=7.83Hz, 2H), 7.439–7.432 (d, J=7.83Hz, 2H), 1.94–1.90 (m, 4H), 1.22–1.04 (m, 18H), 0.86–0.84 (t, J=7.55Hz, 12H). <sup>13</sup>C NMR (125.77 MHz, CDCl<sub>3</sub>):δ ppm 152.49, 139.01, 130.09, 126.13, 121.43, 121.04, 55.64, 53.36, 40.12, 33.90, 32.84, 23.61, 22.64, 14.06.

### **BAF-BA<sub>2</sub>:<sup>3</sup>**

In a 100 ml of two neck round bottom flask a mixture of BAF-Br<sub>2</sub>(4g,7.29 mmol), bispinacolatodiborane (5.56 g 21.88 mmol), KOAc (0.571 g, 5.83mmol), in 1,4-dioxane (30 ml) was degassed before addition of [PdCl<sub>2</sub>(dppf)<sub>2</sub>] (10 mg) and subsequent degassing for 30 min. the reaction was heated under argon at 80° C overnight. After cooling to room temperature, the mixture was extracted with DCM and the organic phase was dried over anhydrous sodium sulfate. After removal of the solvent under reduced pressure, the residue was purified by silica gel column chromatography in hexane to get **BAF-BA<sub>2</sub>** as white solid in 68% yield (3.2g, 4.98 mmol).<sup>1</sup>H NMR (400 MHz, CDCl<sub>3</sub>): δ ppm d 7.86–7.82 (d, J=7.32Hz, 2H), 7.79–7.76 (d, J=7.47Hz, 2H), 7.72–7.69 (d, J=7.47Hz, 2H), 2.03–1.98 (d, J=5.18Hz, 4H), 1.40–1.33 (s, 24H), 0.93–0.72 (m, 16H), 0.69–0.65 (t, J=6.48Hz, 6H) 0.51–0.46 (t, J=7.33Hz, 6H).<sup>13</sup>C NMR (125.77 MHz, CDCl<sub>3</sub>): δ ppm 150.17, 143.94, 133.45, 130.40, 119.24, 83.54, 54.73, 44.00, 34.64, 33.50, 33.47, 27.83, 27.18, 24.83, 22.71, 14.05, 10.34.

### **F2CHO:**

In a 100 ml of two neck round bottom flask a mixture of BAF-BA<sub>2</sub> (0.500 g, 0.778mmol) , BT-F-CHO (0.601 g, 1.94 mmol), K<sub>2</sub>CO<sub>3</sub> (2M Solution 5 mL), in THF (20 ml) was degassed before addition of [Pd (PPh<sub>3</sub>)<sub>4</sub>] (10 mg) and subsequent degassing for half hour. The reaction was heated under nitrogen at 80 °C for 24 hrs. After cooling to room temperature, the reaction was quenched with water and extracted with CH<sub>2</sub>Cl<sub>2</sub>. Organic layer dried over Na<sub>2</sub>SO<sub>4</sub> and the desired compound was purified by column chromatography with hexane, affording brown color semisolid product **F2CHO** in 53% yield (0.350 g, 0.413mmol). <sup>1</sup>H NMR (500 MHz, CDCl<sub>3</sub>): δ ppm 9.76-9.75 (s, 2H), 8.42-8.40 (d,J=7.47Hz, 2H), 8.08-8.03 (m, 4H), 7.97-7.91 (m, 6H), 7.89-7.86 (d, J=7.47Hz, 2H), 2.21-2.14 (m, 4H),0.99-0.85 (m, 20H), 0.59-0.56 (t, J=6.8Hz, 12H).<sup>13</sup>C NMR (75 MHz, CDCl<sub>3</sub>): δ ppm 177.69, 155.25, 154.01, 151.93, 151.87, 151.41, 141.50, 135.82, 128.49, 127.40, 126.44, 125.21, 120.11, 114.12, 44.5, 34.76, 33.86, 28.14, 27.10, 22.15, 13.95, 10.36. FT-IR (KBr) (cm<sup>-1</sup>): 3414, 2921, 2860, 1726, 1673, 1543, 1462, 1388, 1340, 1261, 1218, 1021, 813, 770, 436,406. MS (MALDI-TOF-MS): m/z calcd for C<sub>51</sub>H<sub>50</sub>N<sub>4</sub>O<sub>4</sub>S<sub>2</sub> 847.10; [M]<sup>+</sup>, found 846.35.



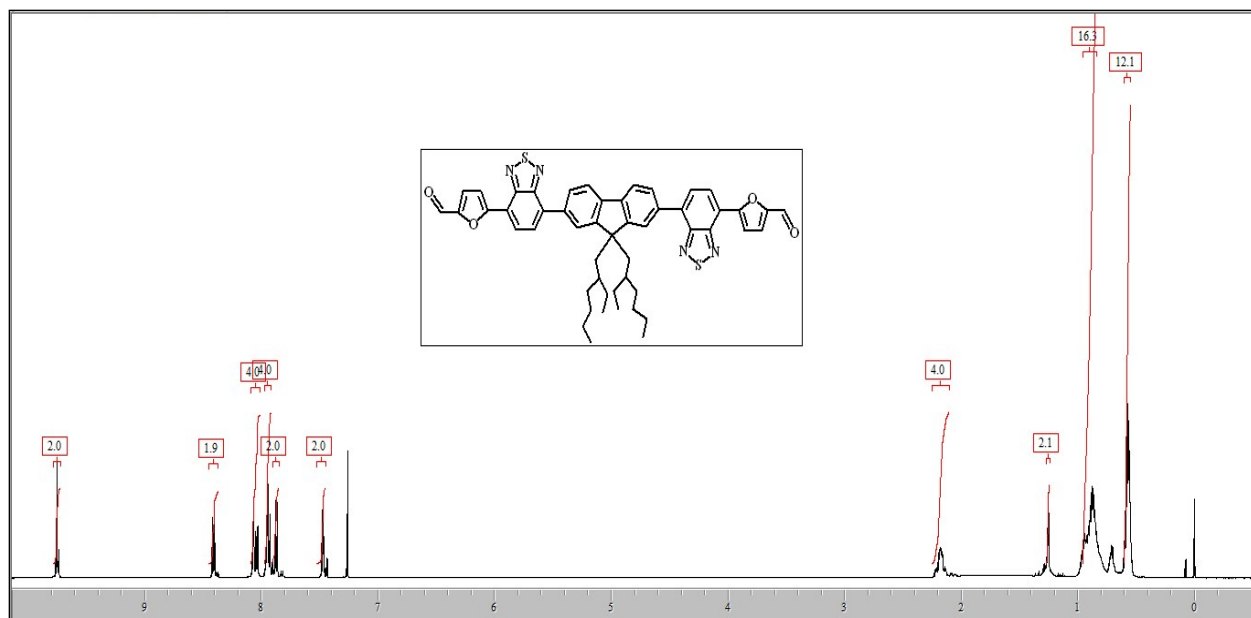


**Fig. S2**  $^1\text{H}$  NMR of F2CHO in  $\text{CDCl}_3$ .

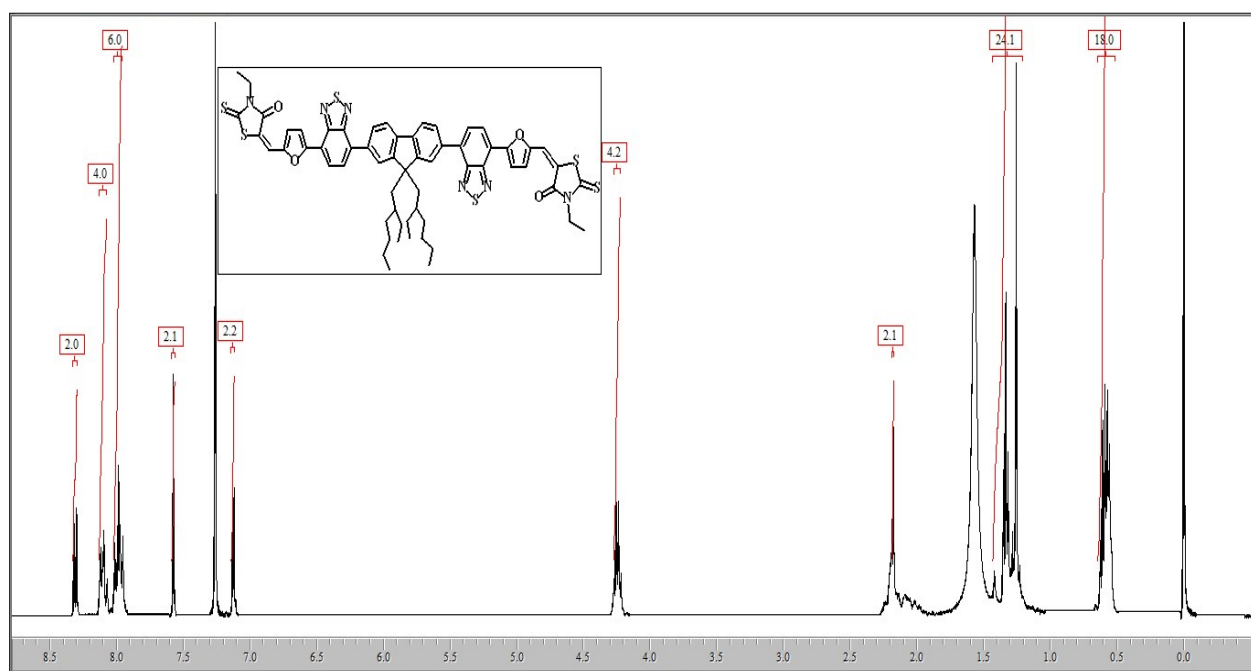


**Fig. S3**  $^1\text{H}$  NMR of FRd<sub>2</sub> in  $\text{CDCl}_3$ .

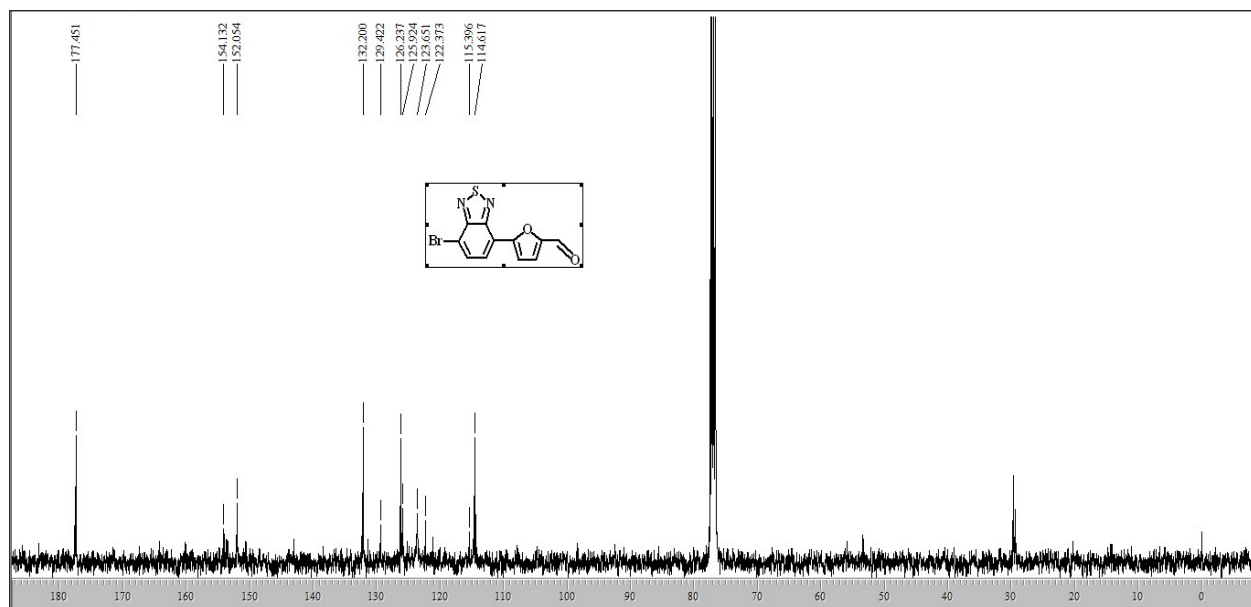


Fig. S4  $^{13}\text{C}$  NMR of BT-F-CHO in  $\text{CDCl}_3$ .

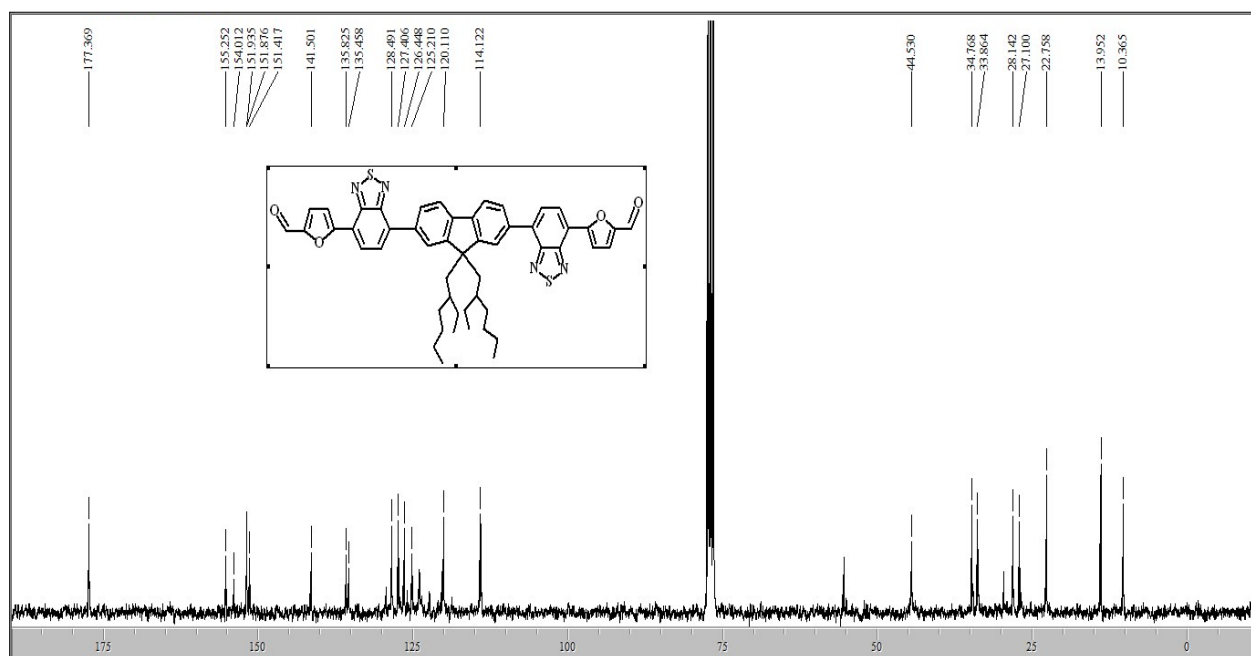


Fig. S5  $^{13}\text{C}$  NMR of F2CHO in  $\text{CDCl}_3$ .

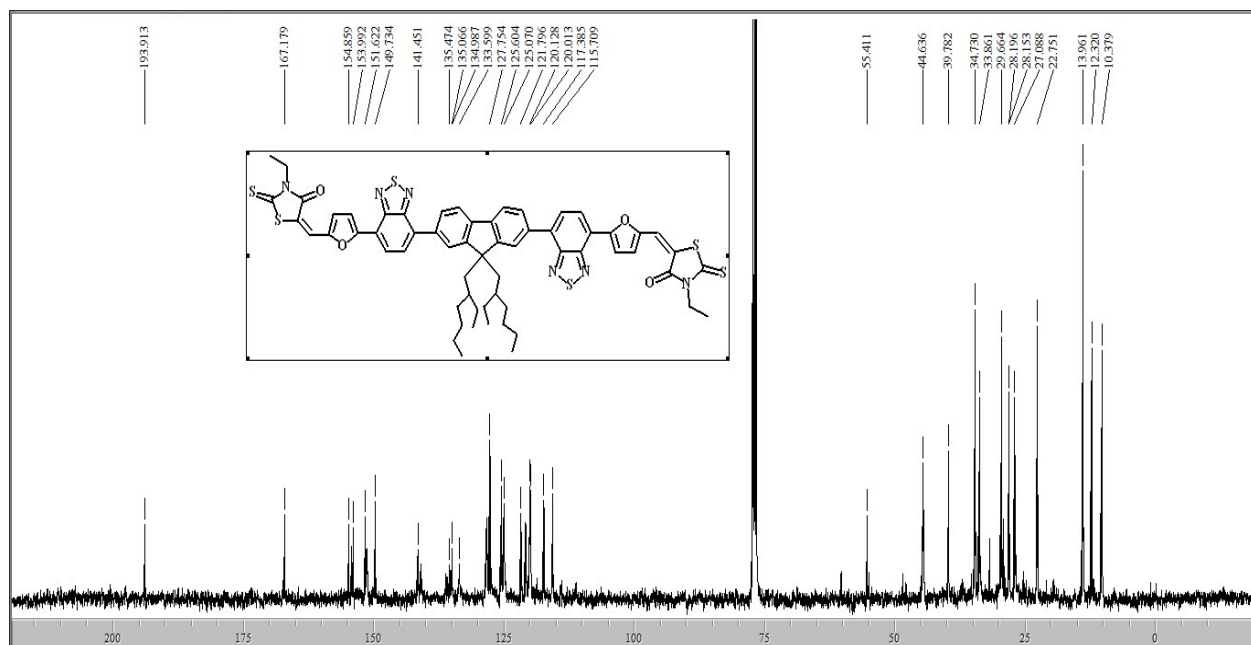


Fig. S6 <sup>13</sup>C NMR of FRd<sub>2</sub> in CDCl<sub>3</sub>

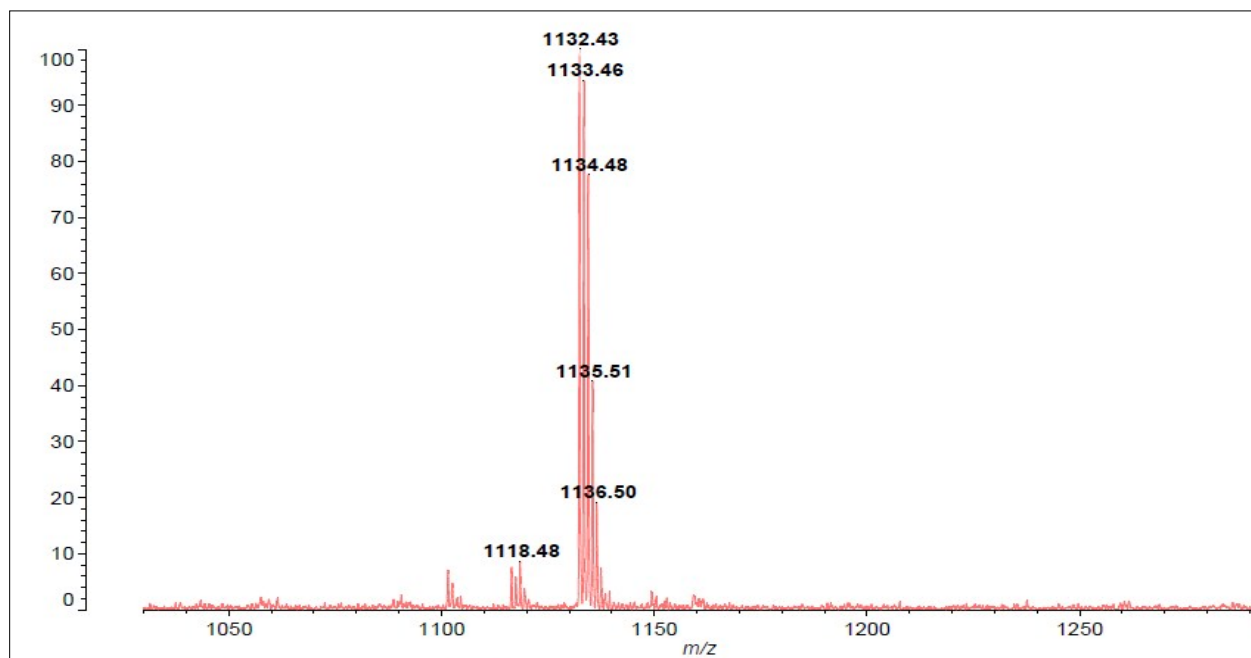


Fig. S7 MALDI-TOF spectrum of FRd<sub>2</sub>.

Indian Institute of Chemical Technology, Hyderabad  
FT-IR Analysis Report

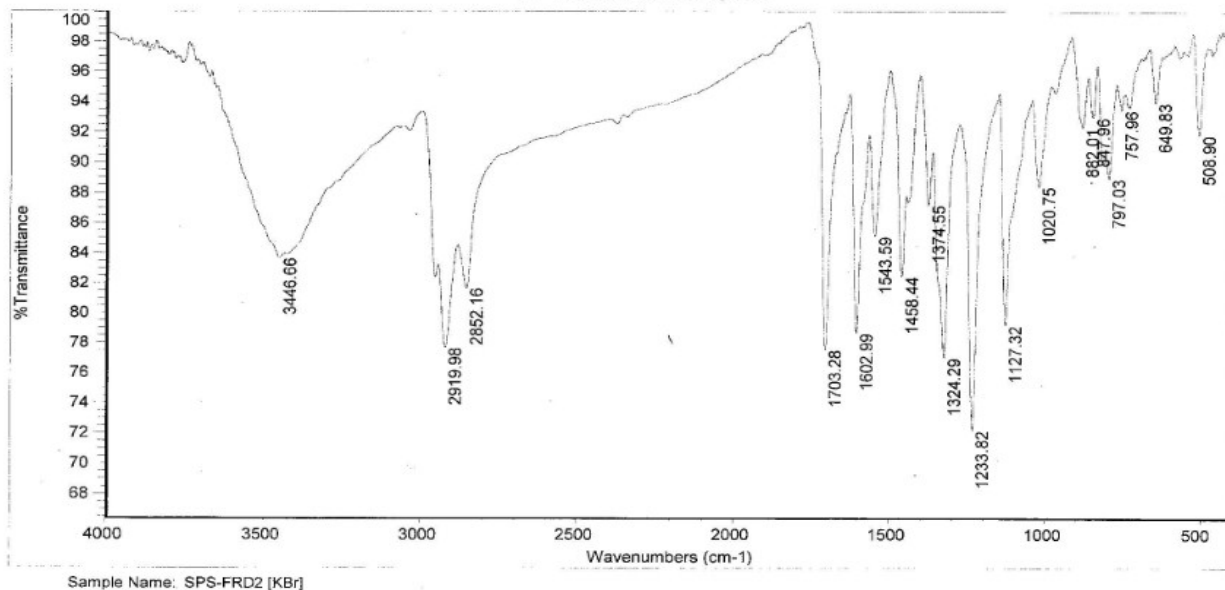


Fig. S8 FT-IR spectrum of FRD<sub>2</sub>.

### S3. Optoelectronic properties

The UV-Vis absorption data of molecule were recorded using a UV-1601 Shimadzu UV-Vis spectrometer. For UV-Vis absorption spectrum in solution, initially a concentrated solution of 0.1 mol·L<sup>-1</sup> in chloroform was prepared, which was further diluted to 0.03 mol·L<sup>-1</sup>. The molar extinction coefficient ( $\epsilon$ ) was obtained from the Beer-Lambert's equation,

$$I = I_0 \times 10^{-\epsilon cl} \quad (\text{S1})$$

where,  $I$  and  $I_0$  are the incident and transmitted light intensity, respectively,  $l$  is the path length, and  $c$  is the analyte concentration. The calculated vs. profile is plotted in Fig. S9. To obtain thin film absorption spectra, first glass substrates were cut into pieces with size of  $1'' \times 1''$ , and then thoroughly cleaned in soap solution and ultra-sonicated in de-ionized water and acetone sequentially for 15 min in each step and dried. To measure thin film absorption spectrum of the molecule, concentrated solutions (15 mg·mL<sup>-1</sup>) in chlorobenzene was prepared and thereafter spin-coated onto clean and dry substrates at 800 rpm for 1 min.

#### S4. Electrochemical properties

The cyclic Voltammogram (CV) measurements were carried out by using a conventional three-electrode cell consisting of a platinum wire working electrode, platinum mesh counter electrode and Ag/Ag<sup>+</sup> reference electrode was in saturated KCl, calibrated against ferrocene as standard. The surface was polished before use and CV measurement was carried out under nitrogen atmosphere at room temperature. The electrochemical cyclic voltammetry was performed in a 0.1 mol·L<sup>-1</sup> tetrabutylammonium perchlorate (TBAP)/dichloromethane (DCM) solution with a scan speed of 0.1 V·s<sup>-1</sup>. A ferrocene/ferrocenium (Fc/Fc<sup>+</sup>) redox couple was used as an external standard. The HOMO energy level was obtained from the onset oxidation potential. The LUMO energy level of molecule was measured by using the equation,

$$E_{\text{LUMO}} = E_{\text{HOMO}} + E_{\text{g,opt}} \quad (\text{S2})$$

while the optical band gap of molecule calculated from the onset of the absorption profile (**Fig. S9**) and electrochemical properties are summarized in **Table S1**.

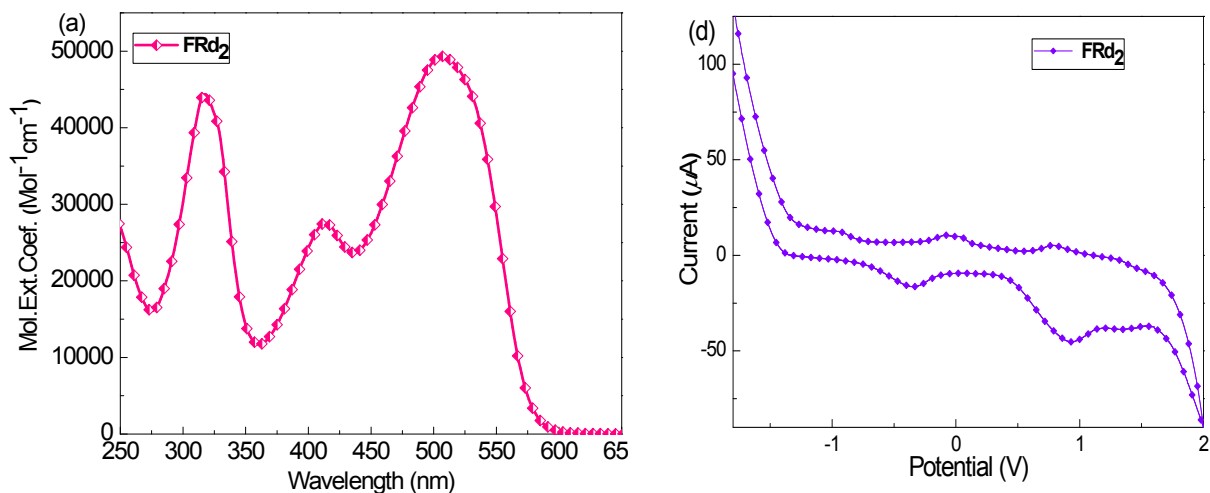


**Fig. S9** (a) Molar extinction coefficient ( $\epsilon$ ), (b) Cyclic Voltammogram of **FRd<sub>2</sub>**.

**Table S1.** Optoelectronic properties of **FRd<sub>2</sub>**.

Molecule	E <sub>HOMO</sub> (eV)	E <sub>LUMO</sub> (eV)	E <sub>0-0</sub> (eV)	λ <sub>max</sub> (solution) (nm)	λ <sub>max</sub> (film) (nm)	ε (Mol <sup>-1</sup> ·cm <sup>-1</sup> )
<b>FRd<sub>2</sub></b>	-5.67	-3.58	2.09	509	511	4.9×10 <sup>4</sup>

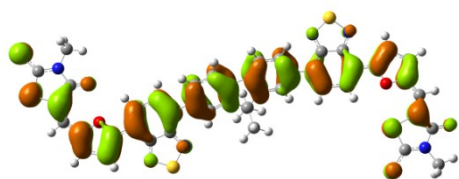
**S5. Density Functional Theory calculation**

To visualize the distribution of frontier molecular orbital levels associated with new donor molecule, ab initio calculations were performed based on time dependent-density functional theory (TD-DFT) at B3LYP level using 6-311g (d, p) basis set in Gaussian software. **Fig. S10** demonstrates the distribution of frontier molecular orbitals of **FRd<sub>2</sub>**. The major allowed transitions in the wavelength range between 300 to 800 nm have been reported in **Table S2**.

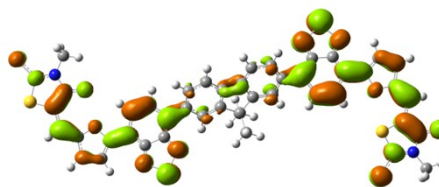
**Table S2.** Major allowed transitions for **FRd<sub>2</sub>** in the range of 300-800 nm calculated at B3LYP/6-311g (d,p) level using density functional theory in DCM solvent.

Transitions	λ (nm)	Osc. Strength	Major contributions
S1	529.4	1.7392	HOMO->LUMO (91%)
S2	485.1	0.0437	HOMO->L+1 (89%)
S3	449.8	0.019	H-1->LUMO (87%)
S4	427.9	0.2306	H-1->L+1 (89%)
S5	396.9	0.2877	H-2->LUMO (11%), HOMO->L+2 (51%), HOMO->L+3 (21%)
S6	378.2	0.3808	H-2->LUMO (79%), HOMO->L+2 (16%)
S7	353.8	0.1077	H-2->L+1 (10%), H-1->L+2 (55%), H-1->L+3 (20%)
S8	350.5	0.0939	H-1->L+2 (16%), H-1->L+3 (66%)
S9	307.1	0.0632	H-7->LUMO (17%), H-6->L+1 (15%), H-2->L+2 (36%)
S10	303.9	0.0577	H-8->LUMO (20%), H-6->L+1 (24%), H-5->L+1 (31%), H-2->L+2 (12%)

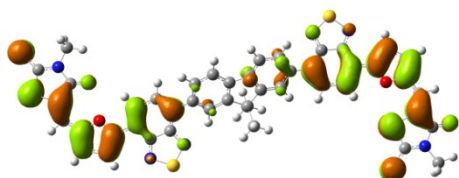
HOMO



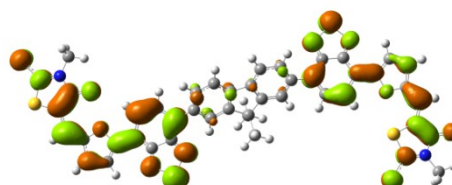
LUMO



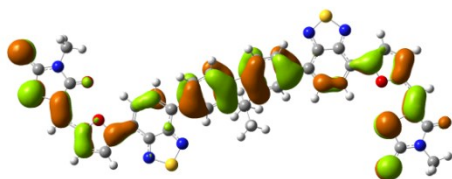
HOMO - 1



LUMO + 1



HOMO - 2



LUMO + 2

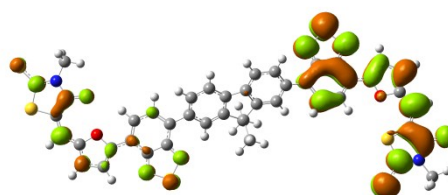


**Fig. S10** Distribution of frontier molecular orbitals of **FRd<sub>2</sub>** as estimated by density functional theory calculation at B3LYP level.

### S6. Device fabrication

The OPV cells were fabricated with inverted device structure Glass/ITO/ZnO/PTB7-Th:**FRd<sub>2</sub>**/*MoO<sub>3</sub>*/*Ag*. The ITO coated glass substrates were cleaned by sequential ultrasonication in detergent containing water, deionized water, acetone and isopropyl alcohol for 15 min in each step. After that the glass substrates were dried under flow of dry nitrogen. The ZnO solution was spin-coated on ITO coated glass substrate at 3000 rpm. Then the film were thermally annealed 200 °C for 1 h on hot plate in air. The solution of PTB7-Th:**FRd<sub>2</sub>** (1:1.5 weight ratio, 25 mg/mL in total weight concentration) in chlorobenzene + additive DIO (3 %) were spin-coated inside the glovebox at 2000 rpm resulting in active layer thickness of 150 nm. Finally, 10 nm thick *MoO<sub>3</sub>* was deposited on active layer and then the top electrode was formed by depositing 100 nm thick *Ag* to complete formation of device.

## S7. Charge carrier mobility

The current density-voltage ( $J$ - $V$ ) curves of ‘hole only’ and ‘electron only’ devices are plotted in log-log scale and fitted with Mott–Gurney’s space charge limited current (SCLC) model,

$$J_{SCLC} = \frac{9}{8} \varepsilon_o \varepsilon_r \mu \frac{V^2}{d^3} \quad (S3)$$

where  $\varepsilon_o$  is the free space permittivity,  $\varepsilon_r$  is the average relative dielectric constant of the blend film and generally taken as 3, and  $d$  is the film thickness. **Fig. S11** and **Fig. 4b** shows the dark  $J$ - $V$  characteristics of those devices treated with thermal annealing and solvent vapor annealing, respectively. The hole mobility of PTB7-Th and electron mobility of **FRd<sub>2</sub>** in blend is found to be higher in case of SVA treated films compared to that of thermally annealed films.

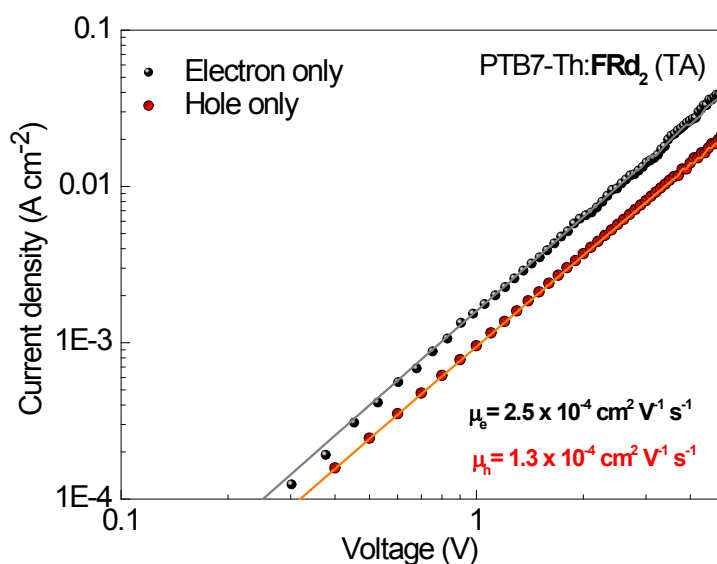


**Fig. S11** Mott-Gurney’s SCLC fitting to calculate hole and electron mobility of PTB7-Th and SMNFEA in thermally annealed films.

**Table S3.** Charge transport parameters of PTB7-Th:FRd<sub>2</sub> blend films.

Treatments	$\mu_h (\text{cm}^2 \text{v}^{-1} \text{s}^{-1})$	$\mu_e (\text{cm}^2 \text{v}^{-1} \text{s}^{-1})$	Ratio
TA	$1.3 \times 10^{-4}$	$2.5 \times 10^{-4}$	1.92
SVA	$2.4 \times 10^{-4}$	$4.3 \times 10^{-4}$	1.79

## S8. Photoluminescence Quenching

Photoluminescence quenching experiments were carried out in order to examine the quenching of PTB7-Th by our new acceptor molecule. As shown in **Fig. 4a** in the main manuscript, PL peak of PTB7-Th at 755 nm is strongly quenched with increasing amount of **FRd<sub>2</sub>**. The PL intensity is quenched about 68 and 91% when the donor-to-acceptor weight ratio in thin film was kept at 1:1 and 1:3, respectively. This finding indicates an efficient exciton dissociation at the donor-acceptor interface. The Stern-Volmer quenching coefficient ( $K_{sv}$ ) has been calculated using the following relation,

$$\frac{\eta_o}{\eta} = 1 + K_{sv}c \quad (\text{S4})$$

where  $\eta$  and  $\eta_o$  are emission efficiency in presence and absence of quenchers, respectively, and  $c$  is the quencher concentration. **Fig. S12** shows the plot of  $K_{sv}$  with respect to acceptor concentration. From the linear fit of data, a  $K_{sv}$  value of  $9.92 \times 10^4 \text{ M}^{-1}$  was obtained.

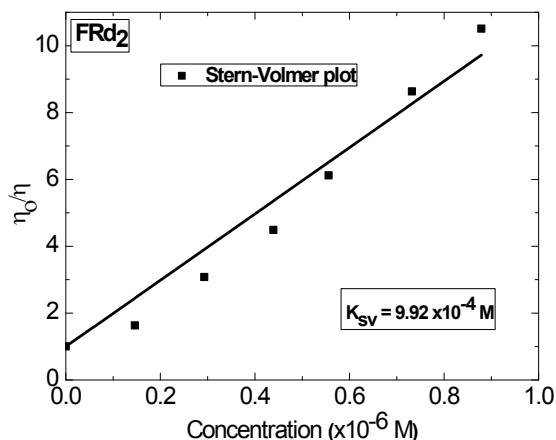


**Fig. S12** Stern-Volmer plots for PTB7-Th:**FRd<sub>2</sub>** blends obtained from PL quenching experiments.

## S9. GIXRD analysis

The micro structural features of pure PTB7-Th and blend film prepared under different experimental conditions were studied by two-dimensional grazing-incidence X-ray diffraction (GIXRD) (**Fig. S13**). The diffraction patterns of PTB7-Th:**FRd<sub>2</sub>** blend films show (h00) lamellar stack spacing  $q \sim 0.14 \text{ \AA}^{-1}$  and (010)  $\pi$ - $\pi$  stack spacing  $q \sim 1.7 \text{ \AA}^{-1}$ . However, there is a significant

increase in the peak intensities for lamellar and  $\pi$ - $\pi$  stacking in the SVA condition of PTB7-Th:FRd<sub>2</sub> blend films. The strong lamellar (h00) and  $\pi$ - $\pi$  (010) stacking peaks are known to improve charge carrier mobility, which in turn lead to better PCE in the case of OSCs.<sup>4</sup>

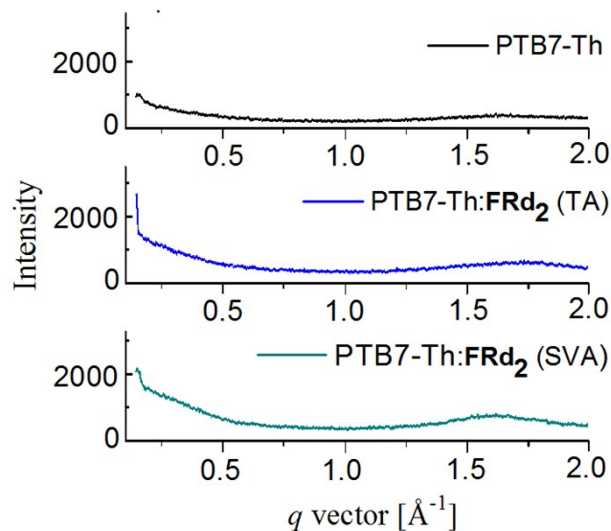


**Fig. S13** The GIXRD graphs of thermally annealed and solvent vapor annealed PTB7-Th:FRd<sub>2</sub> blend film and pristine PTB7-Th films.

## REFERENCES

1. B. A. D. Neto, A. S. A. Lopes, G. Ebeling, R. S. Gonçalves, V. E. Costa, F. H. Quina and J. Dupont, *Tetrahedron*, 2005, **61**, 10975.
2. C. Lavanya Devi, K. Yesudas, N. S. Makarov, V. Jayathirtha Rao, K. Bhanuprakash and J. W. Perry, *J. Mater. Chem. C*, 2015, **3**, 3730.
3. X. Liu, R. Zhu, Y. Zhang, B. Liu and S. Ramakrishna, *Chem. Commun.*, 2008, DOI: 10.1039/b805060k, 3789.
4. Y. Liu, J. Zhao, Z. Li, C. Mu, W. Ma, H. Hu, K. Jiang, H. Lin, H. Ade and H. Yan, *Nat. Commun.*, 2014, **5**, 5293.